Iron and arsenic removal in triple- and single-bed filters: The effects of pH, filtration velocity and filtrate recirculation

Research Project

by

Stelios Flambouris

In partial fulfillment of the requirements for the degree of
Master of Science in Civil Engineering
at the Delft University of Technology

Student number: 4754301
Thesis committee: Prof. dr. ir. L.C. Rietveld, TU Delft
Dr. ir. DJ. de Ridder, Evides Waterbedrijf

TU Delft

Abstract

Arsenic in groundwater can constitute a persistent nuisance for water treatment facilities when it exceeds the admissible limit of 10 μg/L. Recently, a stricter limit has been set as a new challenging target by many companies in the Netherlands, which is below 1 μg/L. However, most of the groundwater treatment plants have been conventionally designed solely for the removal of the most common undesirable groundwater constituents, namely iron, manganese and ammonium. The current research aimed at the investigation of the operational conditions facilitating As removal in biological rapid filters simultaneously with the required Fe removal. This improved As retention should be correlated with an extended length throughout the filter where its adsorption takes place, thus with the deeper Fe penetration inside the bed. Therefore, this was the focus of the current study. The process water used throughout the experimental tests contained $As(III)$ and $Fe(II)$, in order to simulate anoxic groundwater quality conditions. For the most part, a triple-layer filter bed was used, consisted of anthracite, sand and garnet. The different settings under examination involved a range of pH values (7.8, 7.1 and 6.4), two filtration velocities ($2.5m/h$ and $5m/h$) as well as the recirculation of the filtrate back to the feed stream. Finally, the multimedia bed was compared with a single-layer sand filter.

The results of the conducted pilot column experiments revealed that high pH values were accompanied with high oxidation rates and thus with the creation of Fe flocks, already in the supernatant water. Due to this, at pH 7.8 and 7.1 lower Fe concentrations were detected in the effluent, denoting a higher Fe retention as compared to pH 6.4. However, interestingly enough, a relatively deep Fe penetration was observed for every pH value tested. Regarding As removal, it was evidently favored by high pH values owing to the oxidation-floc formation removal mechanism of Fe (homogeneous reaction), which prevailed under those conditions. On the other hand, at pH 6.4 the adsorption-oxidation mechanism was predominant (heterogeneous reaction), which obstructed the AsOB activity. As far as the tested filtration velocities is concerned, they did not seem to significantly impact both Fe spread over the bed as well as As removal at the higher pH levels. Nonetheless, this was not the case for pH 6.4, in which the slow flow rate enabled the generation of more and larger Fe flakes (due to the sufficient residence time in the supernatant water), which were then retained in the top part of the bed. The high flow rate on the other hand allowed Fe to reach deeper in the filter bed. Surprisingly, As removal seemed to be improved at $2.5m/h$, despite the Fe flocks accumulation in the upper layers. Possibly, the short experimental times not allowing equilibrium to be reached, could comprise a reasonable explanation of this unexpected result. Furthermore, the filtrate recirculation stream did not seem to positively influence As removal. The induced dilution effect resulted in a relatively large dispersion of Fe inside the filter bed, however its essentially halved incoming concentration was not sufficient to adsorb the oxidized $As(V)$. Finally, the comparison between the multimedia bed with the single-layer filter reveals a considerably wider Fe dispersion over the bed height in the former case, which in its turn promotes a more efficient As removal.

The overall conclusion of the current study constitutes that triple-layer bed filters facilitate a more gradual Fe removal and its deeper penetration in the bed as compared to single-layer filters. This fact stimulates As removal and additionally allows for longer filter run times. Moreover, heterogeneous Fe removal seems to obstruct As oxidation by AsOB and therefore homogeneous reaction can be considered as more favorable mechanism in terms of As removal. This specific removal mechanism becomes predominant at pH levels above 7, when sufficient oxygen is available. Lastly, the operational setting of filtrate recirculation back to the filter inlet, does not display a positive impact regarding As removal.

Contents

List of Figures

1

Introduction

Groundwater comprises a valuable source of drinking water for many countries in the world. In the case of the Netherlands, approximately 65% of the produced drinking water is coming from groundwater sources [1]. In general, this type of water is considered a reliable source for drinking water purposes and it is for the most part preferred by the water companies, because of its constant and (comparatively to surface water) good natural quality as well as its adequate microbiological quality and stability [2], [3]. As a result, the cost of the required treatment remains relatively low. At the other end of the spectrum, some quality problems are frequently native to groundwater and they are associated with elevated concentrations of iron (Fe), manganese (Mn), ammonium (NH_4), and fluoride (F), whereas sometimes also problems with high concentrations of methane (CH_4), nitrate (NO_3), hydrogen sulphite (H_2S) and arsenic (As) have been reported [3], [4], [5]. The conventional groundwater treatment train consists of aeration followed by rapid sand filtration, targeting mainly at the removal of iron, manganese and ammonium. This is the case in the Netherlands as well, where the water facilities treating groundwater have been entirely designed for the removal of those three main constituents [6]. Nonetheless, in some cases arsenic may comprise a significant nuisance as well and this issue should be taken into account, as it may seriously deteriorate the drinking water quality and pose important public health hazards.

2

Theoretical background

2.1. Arsenic in groundwater

On a global scale, arsenic (As) has been recognized as one of the major concerns regarding groundwater contamination. Especially, in some parts of the world such as Bangladesh, India, Argentina and Mongolia, arsenic problem has been particularly intense and concentrations up to 2000 μg/L in groundwater sources have been reported [7]. Millions of people in Bangladesh and in specific regions of India consume regularly water contaminated by As [8], [9]. Arsenic naturally occurs in over 200 mineral forms. The higher concentrations of the most toxic species amongst them, are more frequently encountered in groundwater sources rather than in surface waters [10]. In general, As is considered to be a highly toxic element and a dosage of 100 mg to 300 mg could be lethal for humans. What is more, As consumption can inflict adverse health effects. This could be the outcome of either acute poisoning or of chronic exposure. Regarding the former, the results could be gastrointestinal effects, haematological abnormalities, renal and respiratory failure as well as pulmonary edema, all of which could potentially lead to shock, coma and in particularly severe cases, even to death [10], [11]. As far as the latter is concerned, As can be blamed for skin lesions, cardiovascular effects and neurological disturbances. Moreover, according to several epidemiological studies, long-term As exposure has been associated with many cancer types, such as skin, lung, bladder, liver and kidney cancer [10], [12]. The aforementioned adverse health effects, induced by As consumption, have led the World Health Organization (WHO), as well as the Environmental Protection Agency (EPA), to adopt a strict guideline value, regarding the maximum admissible concentration of As in drinking water. This upper limit has been set to 10 μg/L [13], [14]. Despite this already low limit, the stimulation of an even further As reduction could potentially bring upon significant benefits in terms of public health and welfare [15]. In that direction, many Dutch water treatment companies evaluate the possibility of setting a new stricter target value, regarding As concentration in the drinking water, namely below 1 μg/L [6].

2.1.1. Arsenic aquatic chemistry

Arsenic in aquatic environments occurs mainly in its inorganic forms and more specifically as trivalent arsenite ($As(III)$) and as pentavalent arsenate ($As(V)$). At near neutral pH and under reductive conditions, As exists predominantly as the electrically neutral H_3AsO_3 (thus as $As(III)$). These are typical conditions of a groundwater source and for that reason under these (anaerobic) conditions, As is mostly encountered in its arsenite form. On the other hand, at neutral pH and under more oxidizing or atmospheric conditions, $As(V)$ is the most common arsenic form, as part of the oxyanions $H_2AsO_4^-$ and $HAsO_4^{2-}$. Figure 2.1 depicts the As speciation as a function of the pH.

There are several techniques and technologies available for the removal of As from water, such as ion-exchange, membrane filtration (reverse osmosis), adsorption on activated carbon as well as co-precipitation after As adsorption onto specific coagulants (e.g. $FeCl_3$ or $Al_2(SO_4)_3$), hydrous ferric oxides (HFO) or iron oxide coated sand [16], [17]. According to Shafiquzzaman et al. [18], As adsorption and its subsequent co-precipitation with iron salts constitutes the simplest and most preferable As removal method.

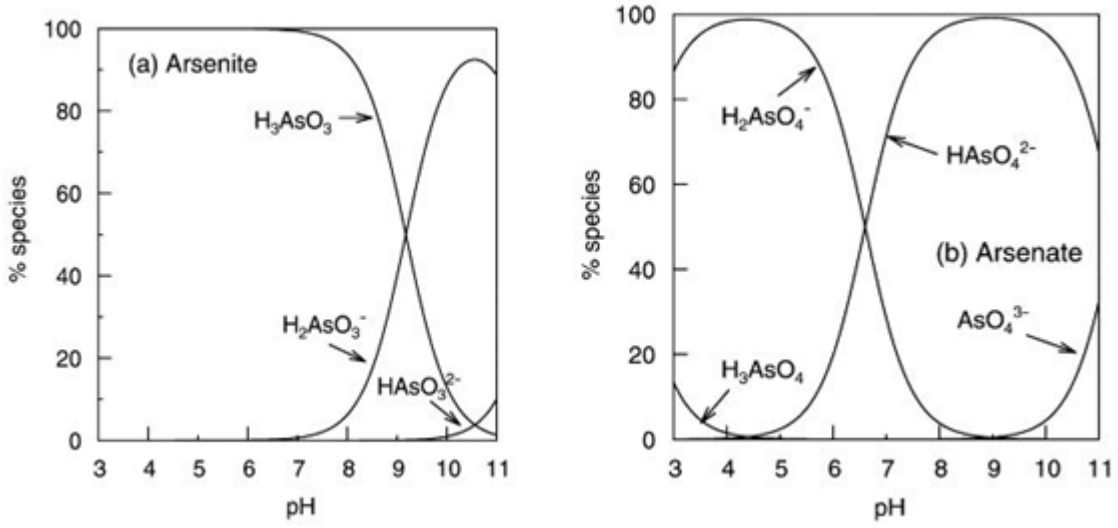

Figure 2.1: Asrenite (left) and arsenate (right) speciation as functions of the pH [7]

2.2. Iron in groundwater

Iron (Fe) is a common constituent of groundwater and this phenomenon can be attributed to the dissolution of iron bearing rocks and minerals in water, during its passing through the subsoil. Although Fe does not pose a direct threat to human health, it constitutes a nuisance for the water supply companies, due to various aesthetic and operational problems associated with it, such as bad taste, staining, discoloration as well as re-suspension in the distribution systems [19]. The proposed guideline of WHO regarding the acceptable Fe concentration in drinking water has been established to a maximum value of 0.3 mg/L [13], whereas the respective mandatory standard for the Netherlands is 0.2 mg/L. What is more, many companies aim at a further decline of the Fe concentration (below 0.03 mg/L), in order to facilitate a superior maintenance of the distribution network and thus to accomplish a considerable reduction in the corresponding costs [20].

2.2.1. Iron aquatic chemistry

Iron in water chiefly occurs in two forms (redox states), namely the reduced soluble divalent ferrous ($Fe(II)$) and the oxidized particulate trivalent ferric ($Fe(III)$) [20]. Under typical anaerobic and reductive conditions (often prevailing in groundwaters), $Fe(II)$ comprises the predominant species. In Figure 2.2, an illustration of the pH-Eh diagram of the aqueous ferric-ferrous system is provided, according to which the iron state in an aqueous system can be estimated as a function of the pH and the redox potential (Eh).

2.2.2. Iron removal mechanisms in rapid sand filters

The conventional way of removing iron from the extracted groundwater entails aeration (cascades, spray aeration, tower aeration) followed by rapid sand filtration. Two types of mechanisms contributing to the removal of Fe in the rapid sand filters could be distinguished, namely the biological and the physicochemical mechanism [20], [22]. Regarding the former, it depends on the activities of specific bacteria capable of oxidizing the dissolved Fe in water, inducing in that way its precipitation under specific pH and redox conditions [23]. Physicochemical mechanism can be further divided into two main sub-mechanisms: floc filtration and adsorptive filtration. Floc filtration or oxidation-floc formation comprises the conventional approach for the removal of Fe, followed by the majority of water treatment facilities [23]. As mentioned above, Fe in anoxic groundwater conditions typically exists as dissolved $Fe(II)$. In the floc filtration mechanism, soluble $Fe(II)$ is oxidized into insoluble $Fe(III)$ forming iron hydroxide flocs, which then can be captured in a sand filter and subsequently be removed from the water stream [24]. The required oxidation of ferrous can be achieved by means of a strong oxidant (e.g. chlorine, ozone) or by aeration. Contrary to the floc filtration mechanism, during the adsorptive filtration or adsorption-oxidation mechanism, Fe is eliminated from water while being in its $Fe(II)$ form.

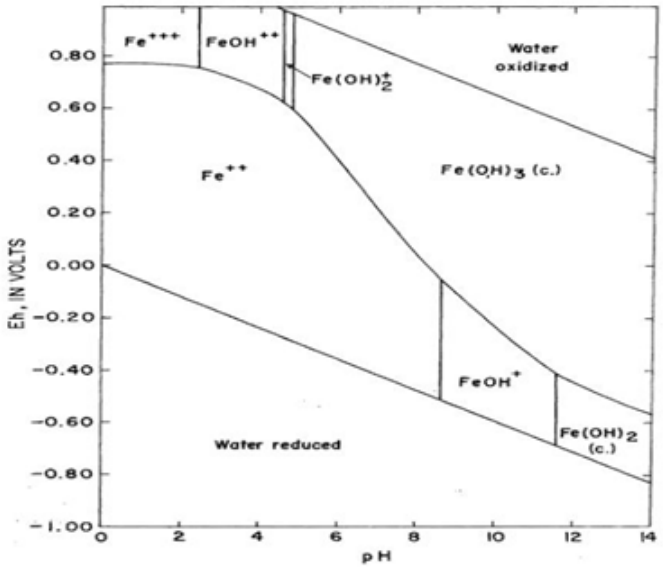

Figure 2.2: pH-Eh diagram of the aqueous ferric-ferrous system [21]

In particular, ferrous is adsorbed onto the grains surface of the filter media and then, in the presence of oxygen, the adsorbed $Fe(II)$ becomes oxidized creating an iron oxide coating, facilitating in that way the additional adhering of new Fe^{2+} ions onto the coating layer [24]. In that manner, the whole process progresses. This kind of mechanism plays a significant role in cases where the pre-oxidation of Fe (prior to its entering in the filter bed) is minimal. Figure 2.3 summarizes the two aforementioned physicochemical iron removal mechanisms.

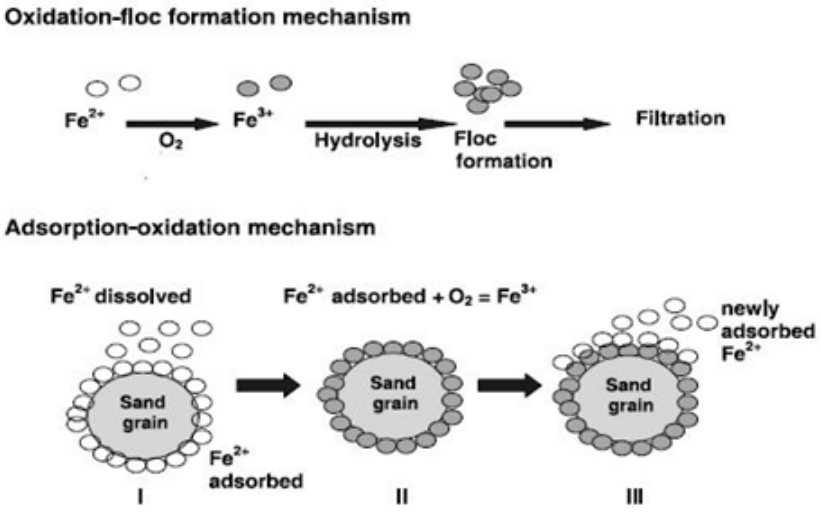

Figure 2.3: Depiction of the physicochemical iron removal mechanisms [24]

The filtration experiments carried out in the context of the current study were based on the floc filtration mode, as will be described in a later part of the report. From the previous analysis, it becomes evident that iron oxygenation kinetics, namely the transformation rate of the soluble Fe^{2+} into the insoluble Fe^{3+} form, constitutes a crucial parameter for the Fe removal in rapid sand filters. The oxidation reaction of Fe^{2+} as well as the subsequent hydrolysis reaction of the newly formed Fe^{3+} ,which results in the formation of hydrated iron oxides, are given below [25]:

$$\textit{Oxidation}: 4Fe^{2+} + O_2 + 2H_2O \rightarrow 4Fe^{3+} + 4OH^- \tag{2.1}$$

$$\textit{Hydrolysis}: 4Fe^{3+} + 4OH^- + 2(x+1)H_2O \rightarrow 2(Fe_2O_3.xH_2O) + 8H^+ \tag{2.2}$$

$$\textit{Overall reaction}: 4Fe^{2+} + O_2 + (2x+4)H_2O \rightarrow 2(Fe_2O_3.xH_2O) + 8H^+ \tag{2.3}$$

This kind of iron oxidation, which takes place mainly in the water bulk solution is termed **homogeneous reaction** and its rate can be described by equation 2.4 [26]:

$$\textit{Homogeneous reaction rate}: \frac{-d[Fe(II)]}{dt} = k_o \cdot [O_2(aq)] \cdot [Fe(II)] \cdot [OH^-]^2 \tag{2.4}$$

, where k_o is the homogeneous iron oxidation rate constant (M/min), $[O2(aq)]$ is the concentration of dissolved oxygen in water (M), $[Fe(II)]$ is the concentration of dissolved ferrous in water (M), $[\mathrm{OH}-]$ is the concentration of hydroxyl ions (M).

Equation 2.4 highlights the important role of pH as operational parameter for the $Fe(II)$ removal. This is because oxidation rate is strongly depended on the pH. Particularly,it increases rapidly at higher pH level, whereas it remains slow at low pH. The critical effect of pH on ferrous oxidation process becomes evident in figure 2.4, retrieved from the study of Stumm and Lee [27]. If sufficient dissolved oxygen is present in the aqueous solution, rapid $Fe(II)$ oxidation takes place at pH values above 7.2.

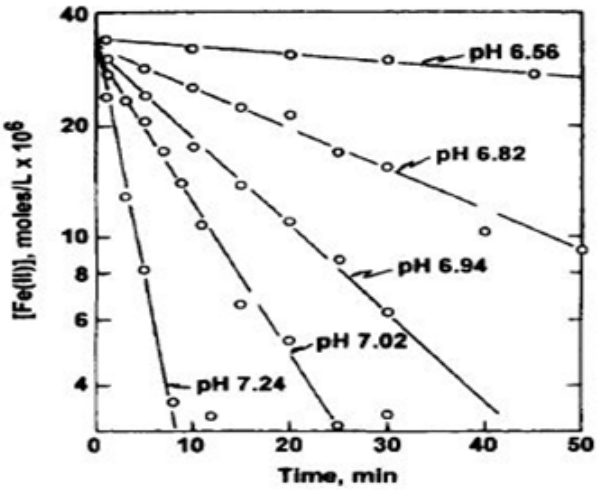

Figure 2.4: Influence of pH on the oxidation rate of ferrous iron [27]

Besides the homogeneous reaction which primarily occurs in the bulk solution, given that proper aeration is provided, another way of $Fe(II)$ oxidation exists. This proceeds via the so called heterogeneous reaction and it is based on the adsorption-oxidation mechanism described above, which means that $Fe(II)$ is adsorbed onto the surface of $Fe(III)$ hydroxide precipitates [23], [28]. In Appendix A.1 the respective equation of the heterogeneous reaction is provided. The catalytic effect of $Fe(III)$ precipitates or iron oxide grains coating on $Fe(II)$ adsorption and oxidation (and hence on the overall removal efficiency) has been reported in previous studies [29], [30]. In a nutshell, three main mechanisms determine the iron removal in rapid sand filters, namely oxidation-floc formation (homogeneous reaction), adsorption-oxidation (heterogeneous reaction) and biological iron oxidation. It is possible that all three mechanisms contribute to the total iron removal at the same time during a filtration process, however which one of them dominates highly depends on the water quality as well as on the specific process conditions [20], [31]. Inside a filter system, a distinguish can be made between the supernatant water

and the filter medium. In the supernatant, primarily the homogeneous reaction occurs whereby the iron flocs are formed, which later on precipitate or get trapped in the filter grains. According to O'Connor [32], the formed precipitates can attract some ferrous particles while they are still suspended in the bulk solution. In that sense, heterogeneous reactions may also occur in the supernatant water. Nonetheless, for the most part heterogeneous reactions take place inside the filter medium, where $Fe(II)$ ions are initially adsorbed onto the surface of the filter grains, they get oxygenated and subsequently they form a coating capable of attracting new Fe^{2+} ions on it. As far as the biological oxidation is concerned, this solely takes place inside the filter bed, as oxidizing bacteria require the medium grains in order to remain attached and to be able to develop. Finally, as mentioned in the previous parts of the current report, oxygen concentration (aeration rate), the pH value of the incoming water, the height of the supernatant water level above the filter bed as well as the filtration velocity comprise decisive factors, that determine which of the aforementioned removal mechanisms will possess the most crucial role during a filtration process [33].

2.2.3. Arsenic - iron interactions

Arsenic removal in naturals waters is widely governed by its sorption onto surfaces of minerals, particulate organic matter and organisms or by biological activity [34]. This situation does not differ significantly in the case of engineered systems. Several treatment technologies aiming at As removal, base their effectiveness on sorption processes. Activated carbon and coagulation with hydrolyzing iron salts comprise such examples [34]. In both natural and engineered systems, hydrous ferric oxides (HFO) possess a key role as major As sorbents. In drinking water treatment processes, HFOs can precipitate in situ during coagulation with $FeCl_3$ or upon oxidation of Fe^{2+} in groundwater and the following creation of HFO-coated sand in rapid sand filters [34]. The adsorption of As on HFOs has been well investigated. Dixitet al. [35] showed that the reduced uncharged arsenite form adsorbs less efficiently on HFOs, as compared to the negatively charged oxidized arsenate form. This may be attributed to the opposite load interactions between the oxyanions of $As(V)$ at near neutral pH (see Figure 2.1) and the normally positively charged iron oxides in the near neutral pH range (see Appendix A.1). However, pH rise can result in decreased $As(V)$ sorption onto HFOs, as at high pH values both the formed iron oxides and the As oxyanions tend to be negatively charged (inducing electrostatic repulsions) [35], [36]. Bissen et al. [37] also concluded that at low As/Fe molar ratios and under limited contact times, As^{5+} adsorbs more effectively on HFOs than As^{3+}.

Based on the above, the importance of As^{3+} oxidation comes to the fore, in order to achieve higher adsorption capacity and subsequently a more efficiently overall As removal. The imperative arsenite oxidation can be sufficiently catalyzed by arsenic oxidizing bacteria (AsOB), which can develop and maintain their population in a filter medium, even at low $As(III)$ concentrations as was reported by the study of Gude at al.[38]. It has been further established that As^{3+} oxidation (and bio-oxidation) primarily occurs in the top part of the rapid filter beds [6]. What is more, a study of Voegelin et al.[39] revealed that $As(III)$ can be partially oxidised by intermittent Fe^{5+} species, during homogeneous Fe^{2+} oxidation. In addition to that, Amstaetter et al.[40] further demonstrated that arsenite oxidation can to some extent also take place inside the sand filters, catalyzed by the heterogeneous Fe^{2+} oxidation occurring onto the iron oxides coatings around the filter grains.

2.2.4. Thesis objective

Objective of the current study comprises the investigation of the interrelated As and Fe behavior inside rapid sand filters, in which As oxidation proceeds via biological activity. As aforementioned, this process chiefly occurs in the top part of the filter bed, transforming arsenite into the oxidized arsenate. Since $As(V)$ is efficiently adsorbed onto HFOs, the penetration of iron flocks deeper into the filter bed has been hypothesized to positively affect As removal. Another reason justifying the targeted larger spread of HFOs over the entire filter bed height, lies in the hypothesis that Fe flocks captured in the top layer could obstruct the proper development and performance of the AsOB. In this research, the desired Fe penetration was tested by means of different operational conditions, involving different filter media layers, filtration velocities, pH values as well as investigation of the filtrate recirculation effect. All in all, the effects of these operational parameters on both the Fe as well as the As removal state, comprise the subject of the current study.

3

Materials and Methods

At first, it should be be highlighted that the experimental work performed in the context of the current study constitutes a part of a larger scientific process, which lasted for about seven months and aimed at the investigation of the appropriate operational conditions, which would enable the deeper iron flocs penetration into the rapid filter bed and the subsequent maximization of arsenic removal.

3.1. Process water quality

The water used in the experimental procedure was Delft's tap water, which was stored in a basin for some days prior to its usage. Delft's tap water quality is given in Table 3.1. The displayed values comprise averaged values of a two-month period (September/October 2018) provided by Evides Waterbedreijf. As this water was not directly used for the experimental purposes, minor discrepancies between the quality given in Table 3.1 and final process water's quality might be occurred.

3.2. Pilot column set-up

The experimental set-up is depicted in figure 3.1. This was located in the WaterLab of the CEG building, at TU Delft, where all the experiments took place. The set-up consisted of six identical columns and it was designed so that three duos were running at the same time in duplicates. Each column had a diameter of 8.5 cm and a height of 1.5 m. The filter bed itself occupied 1 m of the column's height and it comprised three different layers from the top to the bottom: 40 cm of anthracite (2 - 4 mm), 40 cm of coarse sand (1.4 - 2 mm) and 20 cm of garnet (0.7- 1.4 mm). Over the course of the experimental process, two of the mixed-bed columns were replaced by two single-layer filters, comprised of coarse sand grains (0.8 - 1.2 mm). The necessary sampling along the filter bed was realized by means of ten sampling points situated every 10 cm. Additionally, all columns could be disconnected halfway

Table 3.1: Delft tap water quality (Evides Waterbedrijf)

Tap water quality parameters	Units	Values
Temperature	°C	10
pH	[-]	8.05
Electrical conductivity	mS/m	46
Total hardness	mmol/L	1.42
O_2	mg/L	7.5
Fe	μL	<5
SO_4	mg/L	49
Mg	mg/L	7.1
Mn	μg/L	<0.4
ATP	ng/L	3.5

Figure 3.1: The pilot column set-up used for the experiments

rendering its content more accessible to sampling. The rest of the parts making up the experimental set-up comprised circulation pipes, a dosing pump, four reservoirs containing the chemical solutions dosed in the system, recirculation and effluent tanks as well as a mechanical system for controlling the supernatant water level, which was composed by a float, pulleys and a movable overflow in the effluent side. Regarding the level of the supernatant water, it was initially set at about 25 cm above the filter bed surface, however due to the ongoing filter clogging, it could rise up to 50 cm (overflowing situation), just before the backwashing. Backwashing was executed using tap water coming from a hose connected to the bottom of the column. During backwashing, filter beds were expanded by 25% over a time period of about 15 min and up to the point that supernatant water was visually clear. As far as the influent water flow rate is concerned, it could be manually regulated by a valve placed in the feed pipe on the top part of the set-up. Similarly, the recirculated flow was also regulated by means of a manual valve placed in the recirculation pipe. Finally, the dissolved $As(III)$ was dosed by a central reservoir to all the columns simultaneously, whereas dissolved $Fe(II)$ was supplied by three different tanks to each of the three duos separately (achieving in that way the desired different pH values according to the different acid dosing in the respective tanks). The schematic overview of the a single filter column setup is illustrated in Figure 3.2.

3.3. Experimental settings and plan

During the experimental process, multiple designs and operational conditions were tested. More specifically, the following settings were examined: 1) three pH values, 6.4, 7.1, 7.8, 2) two filtration velocities, $2.5m/h$ and $5m/h$, 3) the impact of a $2.5m/h$ filtrate recirculation stream (resulting in a total filtration velocity of $5m/h$) and lastly 4) two different filter media (single-bed and mixed-bed filters). Prior to those trials, a necessary 3 month period preceded, involving the pilot build-up and start-up, the inoculation of the filters as well as a sufficient biological phase which resulted in the development and accumulation of the required biomass. Over that period, all columns experienced preloading with process water, containing 20 µg/L $As(III)$ at a filtration rate of 5 m/h. Table 3.2 presents a complete and supervisory overview of the total experimental plan.

In more detail, after the initial ripening phase ($Period1$), all columns continued to operate under the constant feed flow of 5 m/h, while the respective pH values were the ones shown in Table 3.2. Samples for the determination of As and Fe concentrations were collected during that period ($Period2$), which lasted for about two weeks. Afterwards ($Period3$), the filtration flow was halved (2.5 m/h) in all the

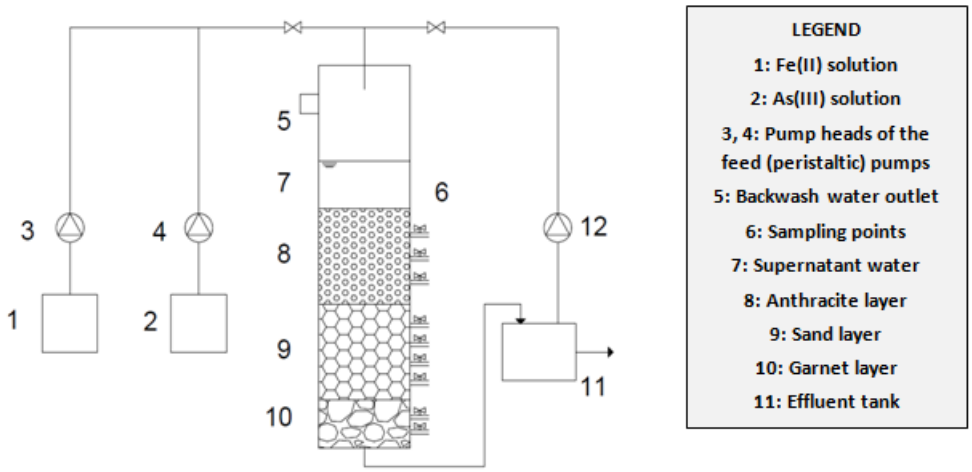

Figure 3.2: Schematic overview of a single pilot column

columns, while keeping the other parameters unchanged, investigating in that way the influence of filtration velocity over As and Fe removal. After the 20 days of $Period3$ had passed, the columns of duo 1 were emptied, filled with coarse sand and left to be ripened. The filtration velocity for this pair was set at 2.5 m/h, whereas the incoming water was acidified to the pH value of 7.1. At the same time, the velocity of the rest of the columns increased again to 5 m/h, but this time half of the flow was provided by the recirculation of the filtrate. The recirculation was realized by means of a small submergible pump in the effluent tank. Those experimental conditions were held for two weeks ($Period4$). Once the ripening of the sand containing filters had sufficiently progressed, samples started to be taken for a period of one week. The incoming water pH was maintained at 7.1. During the same week ($Period5$), the filtrate recirculation applied to the other two duos was terminated and a second run of trials with filtration velocity 2.5 m/h commenced. Over the last experimental period ($Period6$), samples were continued to be collected from the single-layer duo, but in that occasion at a lower pH value (6.4). Finally, aiming at verifying the biological nature of As oxidation, the multimedia beds were disinfected by chlorinated water for two days and afterwards samples were received and analyzed.

3.4. Experimental procedure and analytical methods

The experimental procedure entailed the collection of water samples from several sampling points (small taps in Figure 3.2) along the columns' height and their subsequent quality analysis in terms of As and Fe concentrations. In particular, the first sampling point concerned the incoming water and therefore it was placed just above the filter bed. Then, 5 samples were received from the water flowing through the filter beds, every 10 cm (from top to the bottom). The last sample concerned the effluent water (filtrate). Regarding the backwashing process, a stabilization period after each rinsing of at least 24 hours was maintained, before the next sampling run. In addition, although the clogging rate was not identical for all the columns, all of them were backwashed simultaneously in order to preserve the uniformity of the AsOB biofilm among the different duos. Evidently, the fastest blocking column was the normative one. Once the required samples had been collected, their quality analysis procedure succeeded. Particularly, from every single sample, three types of sub-samples were obtained (by using a syringe and a pipette): 5 ml of unfiltered, 10 ml of 0.45 μm filtered and another 10 ml of both 0.45 μm filtered and As-speciated samples. The filtration was realized via a 0.45 μm Whatman syringe filter, whereas the As speciation was accomplished by forcing the filtered water to pass through an anionic ion-exchange resin (Amberlite® IRA-400 chloride form), capable of retaining the charged $As(V)$ species and thus allowing the uncharged $As(III)$ species pass through it. Regarding the filtered sub-samples, they were considered to contain only dissolved $Fe(II)$, since the $Fe(III)$ flocs were blocked by the filter. The analysis of the unfiltered sub-samples was realized spectrophotometrically (by the photometric 0.0025 - 5 mg/L Fe Spectroquant® method), achieving the determination of their total Fe content. The other two (filtered and filtered and As-speciated) sub-samples were analyzed by means of Inductively Coupled Plasma Mass Spectrometry (ICP-MS). In that way, total As, $As(III)$ as well

Table 3.2: Overview of the total experimental plan

Period 1	Biological ripening time		
Period 2	Filtration velocity (only feed) [m/h]	pH [-]	Filter bed [-]
Column duo 1	5	7.8	Triple-layer
Column duo 2	5	7.1	Triple-layer
Column duo 3	5	6.4	Triple-layer
Period 3	Filtration velocity (only feed) [m/h]	pH [-]	Filter bed [-]
Column duo 1	2.5	7.8	Triple-layer
Column duo 2	2.5	7.1	Triple-layer
Column duo 3	2.5	6.4	Triple-layer
Period 4	Filtration velocity (feed + recirculation) [m/h]	pH [-]	Filter bed [-]
Column duo 1	-	-	-
Column duo 2	2.5 + 2.5	7.1	Triple-layer
Column duo 3	2.5 + 2.5	6.4	Triple-layer
Period 5	Filtration velocity (only feed) [m/h]	pH [-]	Filter bed [-]
Column duo 1	2.5	7.1	Single-layer
Column duo 2	2.5	7.1	Triple-layer
Column duo 3	2.5	6.4	Triple-layer
Period 6	Filtration velocity (only feed) [m/h]	pH [-]	Filter bed [-]
Column duo 1	2.5	6.4	Single-layer
Column duo 2	Chlorination (2.5 m/h)	7.1	Triple-layer
Column duo 3	Chlorination (2.5 m/h)	6.4	Triple-layer

as $Fe(II)$ concentrations were measured. Based on that, $As(V)$ and $Fe(III)$ concentrations could be calculated. This was done by subtracting $As(III)$ and $Fe(II)$ concentrations from the respective total measured As and Fe concentrations.

Complementary to the previously described measurements, a PAMAS particle counter (10 channels, size range 1-20 μm) was employed, whereby the particles cumulative volume (for some indicative unfiltered samples) was determined. Last but not least, after the completion of the total experimental process, the columns were drained and emptied from their contents, whereas some representative samples of the filter medium grains were kept and subsequently analyzed by means of an optical microscope (KEYENCE VHX-5000 Digital Microscope).

3.5. Chemical solutions

The required $Fe(II)$ and $As(III)$ solutions were prepared using the reagents $FeSO_4.7H_20$ (Sigma-Aldrich) and As_2O3 (Sigma-Aldrich), respectively. These were diluted in the process water up to the desired concentrations. Afterwards, the prepared solutions were dosed into the supernatant water targeting at the influent concentrations of 2 mg/L $Fe(II)$ and 20 μg/L $As(III)$ for each individual column. Regarding the desired pH, it was reached by adding the appropriate amount of H_2SO_4 (96% Sigma-Aldrich) to the tanks containing the $Fe(II)$ solutions. The $As(III)$ solution was placed in a separate plastic container from which it was distributed to all the columns simultaneously.

4

Results and Discussion

4.1. Biological ripening of AsOB filters

Prior to the main experimental process initiation, the growth and maturation of the AsOB was imperative to be verified. For this to be done, total As as well as $As(III)$ concentrations analysis was performed. Samples collection started about one month after the columns filling. The averaged results of three samplings over a seven-week period are presented in Appendix A.3. In all cases, the majority of As present in the filtrate was in its oxidized form ($As(V)$), indicating microbial activity. It appears that in duos with higher pH values (7.8 and 7.1), the oxidation process proceeded somewhat faster as compared to the lower pH duo (6.4). It was also shown (results not presented here), that arsenic oxidation was already underway after one month of columns ripening. Moreover, it is worth noting, that over the course of the ripening process, the most intense As oxidation was observed on the top 30 cm of the biological columns. This observation is in line with previous studies, which highlighted that the main AsOB activity occurs in the top part of the filter beds [41]. Finally, the graph of Appendix A.3 shows that a limited amount of total As seems to be removed. This can be attributed to the limited adsorption of $As(V)$ onto the filter grains. All in all, As analysis revealed the existence and maturity of the AsOB in the filter beds, evinced by the fact that the majority of As undergone sufficient oxidation inside the columns, while this happened predominantly in their upper part.

4.2. Effect of pH on As and Fe removal

After the AsOB development was confirmed, the main experimental process, aiming at investigating the common As and Fe removal, commenced according to the plan presented in Table 3.2. The total Fe concentration profiles along the filter beds height, at different pH values (corresponding to the three different duos) with the filtration velocity 5 m/h are depicted in Figure 4.1. For the creation of those graphs, the duplicate columns as well as the four-days measurements over a period of nine days were averaged. It can be observed, that higher pH values are accompanied with lower Fe concentrations in the effluent, which is directly related to the higher oxidation rates and the subsequent $Fe(III)$ flocs formation. These, in their turn, are captured in the filter medium pores. Based on this, it would be anticipated that those flocs would be retained in the top part of the bed and consequently they would not reach the deeper layers, at least in significant amounts. Nevertheless, contrary to this hypothesis, at pH 7.8 Fe seems to penetrate deeper in the bed. A potential explanation could be, that the formed $Fe(III)$ flakes broke up inside the filter bed into smaller particles whereby they managed to pass through the filter's pores and be present in high depth in the column. Regarding the lowest pH case, Fe retention comes primarily from the heterogeneous reaction of the dissolved Fe onto the filter media grains. The variations in the oxidation rates at different pH values become glaringly obvious from the graphs presented in Appendix B. As can be seen there, in columns treating high pH water, nearly all the amount of Fe enters the filter bed as particulate $Fe(III)$, due to its prior oxidation in the supernatant water. This fact evidently facilitates its removal inside the bed. On the other hand, at low pH, the greatest part of Fe remains dissolved and in that way it can more easily escape via the effluent.

The respective total As concentration profiles with the same filtration velocity (5 m/h) are illustrated in Figure 4.2. The samples used for the production of the graphs of Figure 4.2, were the same as

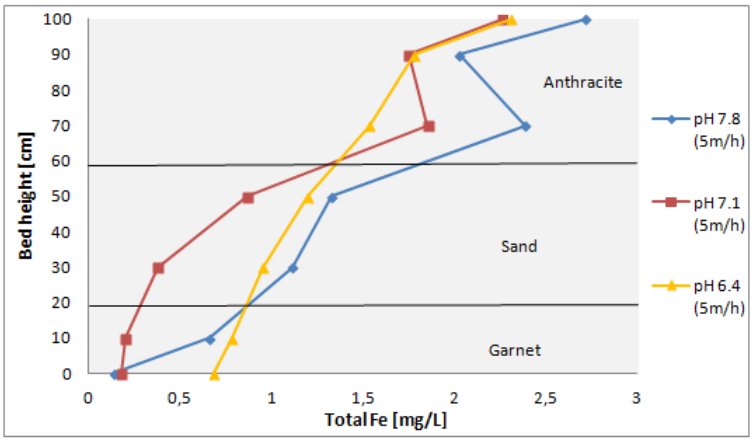

Figure 4.1: Total Fe concentration profiles over the filter bed height with the filtration velocity 5 m/h

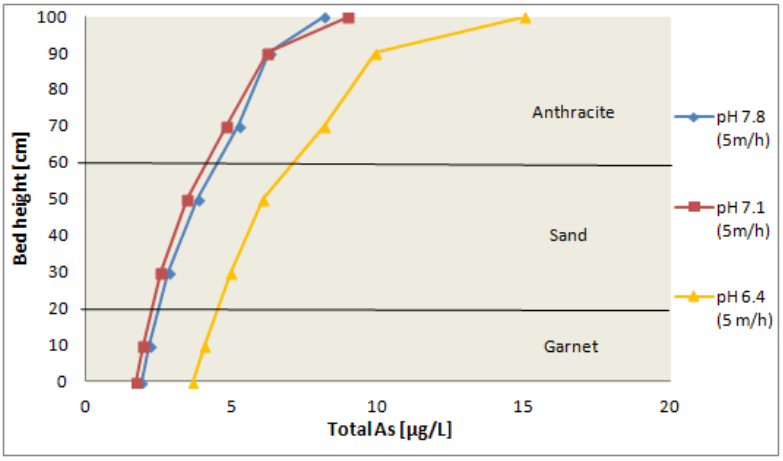

Figure 4.2: Total As concentration profiles over the filter bed height with the filtration velocity 5 m/h

for the Fe profiles case. As removal pattern appears to be identical for the high pH duos, while at pH 6.4 the removal efficiency was consistently lower. Possibly, this was the outcome of the AsOB hindrance by the heterogeneous Fe removal, due to the grains surface coverage by the adsorbed iron. Additionally, in the low pH range the majority of iron lay in its dissolved form (see Appenix B) and as a result only a limited amount of $Fe(III)$ flocs existed, capable of absorbing arsenic. Another important feature comprises the fact, that the amount of As leaving the filter bed via the effluent existed primarily as $As(III)$. The respective results are shown in the graphs of Appendix C. These results are in perfect agreement with the previous discussion, namely $As(III)$ adsorbs less efficiently onto HFO flocs and coatings, as compared to $As(V)$ and thus it is normally less removable.

4.3. Effect of filtration velocity on As and Fe removal

The following experimental series involved the reduction of the filtration velocity in half (2.5 m/h) in all the examined columns and the study of the resulting effect in terms of As and Fe removal. In Figure 4.3, total Fe concentration profiles over the three different duos for the applied filtration velocity 2.5 m/h are illustrated (solid curves). Those graphs were based on averaged values of the duplicate columns sampling results, along with the averaged measurements of four samplings over a two-week period (thus, in total eight samples per column duo were averaged). For comparison purposes, Fe profiles at 5 m/h (at pH 7.1 and 6.4) are plotted as well (dashed curves). At the highest pH values, filtration velocity seems to play a minor role in Fe penetration and removal, since those profiles display similar patterns at both 2.5 m/h and 5 m/h. However, an important variation occurred for pH 6.4. In that case, where oxidation rate is low, the residence time of Fe in the supernatant water appears to be

highly important. Particularly, for 2.5 m/h the Fe residence time and subsequently the contact time with oxygen was considerably higher as compared to double that flow rate and thus more and larger $Fe(III)$ flakes could form, before Fe encountered the filter grains. Hence, as it would be expected, at slow flow rate most of the Fe was retained in the top part of the bed. According to Figure 4.3, about 58% of total Fe had already been removed in the first 10 cm of the bed and more than 74% in the upper 30 cm. On the other hand, the high flow rate did not allow for long residence and contact times, resulting in primarily dissolved Fe entering the filter bed and rendering heterogeneous reaction the main removal mechanism. As can be seen, under those conditions, Fe penetrated deeper in the bed and higher concentrations could be detected in the filtrate.

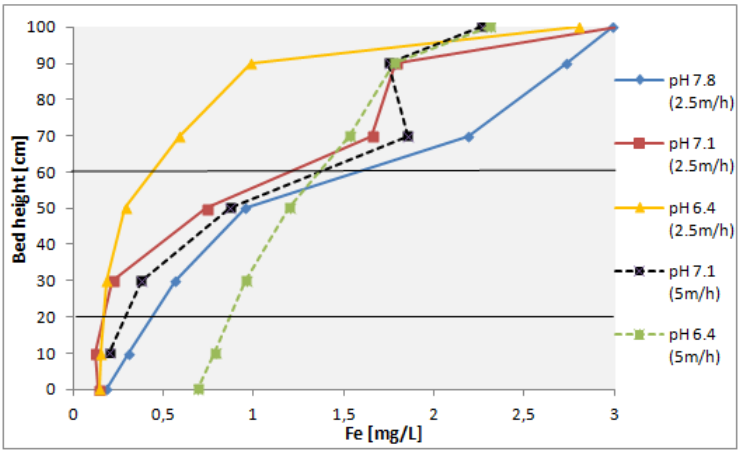

Figure 4.3: Total Fe concentration profiles over the different columns when filtration velocities of 2.5 m/h (solid curves) and 5 m/h (dashed curves) were applied

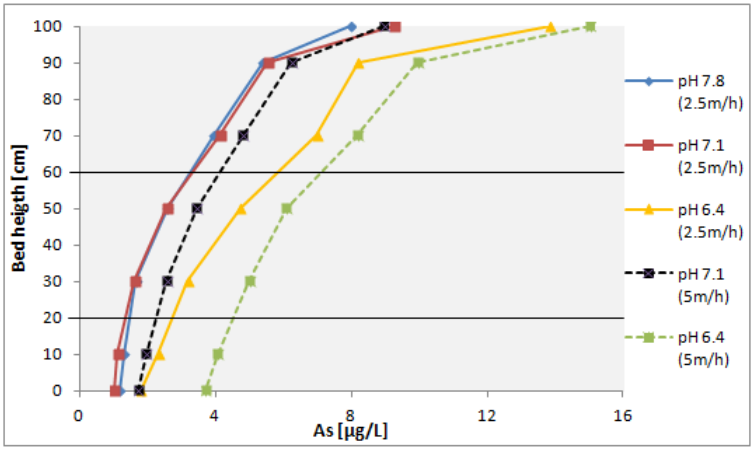

Figure 4.4: Total As concentration profiles over the different columns when filtration velocities of 2.5 m/h (solid curves) and 5 m/h (dashed curves) were applied

The exact same samples analyzed to create the Fe profiles, were also used for the production of the total As concentration profiles, illustrated in Figure 4.4. The alteration of the flow rate, did not heavily impact As removal at the highest examined pH values, as at both pH 7.8 and 7.1 As removal follows identical patterns, although it appears slightly improved for 2.5 m/h. As far as pH 6.4 is concerned, again As retention was consistently higher at 2.5 m/h than at 5 m/h. In Appendix D, all the one-to-one Fe and As profiles for 2.5 m/h and 5 m/h are presented, facilitating the comparison between the two flow rates for each pH value. Finally, from the aforementioned, it appears that As removal efficiency was somewhat higher in the case of 2.5 m/h at all the examined pH values, which contradicts what would be expected, since at 5 m/h iron's spread over the filter bed was larger. Especially, at pH 6.4, this discrepancy becomes even more evident, since in that case Fe penetration at 5 m/h was considerably

larger than at 2.5 m/h. A potential explanation of this unexpected behavior could lie in the experimental conditions themselves. More specifically, the time period over which experiments run at 5 m/h, was shorter than the respective time period for experiments at 2.5 m/h (which was maintained for 20 days). Thus, the stabilization time was probably not sufficient for equilibrium to be reached, contrary to what was the case for the 2.5 m/h tests.

4.4. Effect of filtrate recirculation on As and Fe removal

The next operational setting under investigation involved the recirculation of part of the filtrate back to the inlet stream. The total flow rate was 5 m/h, 50% of which was provided by the feed flow (2.5 m/h), whereas the rest 50% by the recirculated filtrate (2.5 m/h). For this set of experiments, only the duos at pH 7.1 and 6.4 were sampled and analyzed. The resulting total Fe and total As concentration profiles are demonstrated in Figures 4.5 and 4.6, respectively. Their production was based on averaged results retrieved from samples of the duplicate columns (for each of both duos) as well as of five-days measurements over a two-week period. The total Fe concentration of the process water flowing through the different heights of the filter bed are shown in Figure 4.5. To start with, there was a clear dilution effect induced by the recirculation flow, because the filtrate contained only a small amount of Fe. Essentially, in that way the incoming Fe concentrations were halved. Regarding Fe removal, a similar pattern can be observed at both pH 7.1 and 6.4 in the mixed stream (feed + recirculate), although in the case of the latter more iron could be detected in the deeper layers of the bed. At pH 7.1 and in the middle of the bed, about 71% of Fe had been removed, while at pH 6.4 the respective percentage nearly approached 49%. What is more, it seems that Fe was for the most part evenly distributed over the bed height. Similarly, when solely feed flow was applied (no filtrate recirculation), a comparable gradual Fe removal along the filter bed height could be observed. In that case, the retained amounts in the middle of the bed at pH 7.1 and 6.4 comprised 61.6% and 48.2% of the total incoming Fe, respectively. Of course, the Fe concentrations in that occasion were higher throughout the bed, due to the lack of the dilution effect.

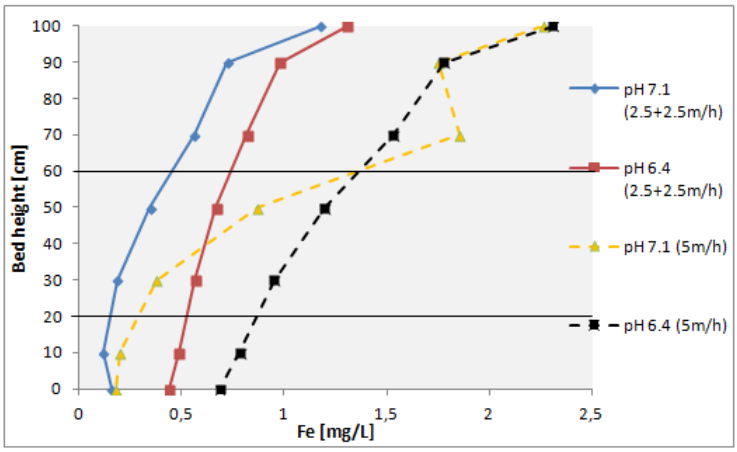

Figure 4.5: Total Fe concentration profiles over the different columns when 5 m/h filtration velocity with (solid curves) and without (dashed curves) filtrate recirculation was applied

Figure 4.6 illustrates that As removal profiles, when recirculation was applied, followed roughly similar patterns with the respective Fe removal profiles. It seems, that at pH 6.4 As removal delayed as compared to the higher pH value, although in the effluent ultimately both of them reached the same level. This delay in As removal coincided with the presence of higher Fe concentrations (at pH 6.4), which theoretically would not be expected. However, as shown previously, most of the Fe at pH 6.4 was present as dissolved $Fe(II)$ and consequently its removal mechanism proceeded via the heterogeneous reaction, on the surface of the filter medium grains. This type of mechanism potentially hindered the As oxidation process realized by the AsOB, due to the competition for the grains surface. On the other hand, at pH 7.1 effectively the whole amount of Fe entered the filter bed as particulate $Fe(III)$ flakes and thus no coverage of the grains surface took place. From the graphs in Appendix E, the discussed variation in the form of Fe entering the filter bed as a function of the pH, for the case of the

recirculation mode, can clearly be noticed. However, except for the potential As oxidation obstruction by the heterogeneous Fe removal, the Fe form itself can have an effect on As removal. Particularly, $Fe(III)$ flocks can directly adsorb $As(V)$ and to some lesser extent $As(III)$. So, once again, it can be concluded that the proportion of Fe that has been oxidized comprises a key factor towards As removal enhancement.

Graphs depicting As speciation over the bed height for both settings under investigation (with and without recirculation) are also provided in Appendix E. It comes out, that the majority of As comprised $As(III)$. This means, that once $As(V)$ formed, it was directly adsorbed by the HFOs in the bed. Also, this phenomenon was more rapidly occurred at pH 7.1, since under those conditions more HFOs had been created. Concerning pH 6.4, a relatively large amount of oxidized $As(V)$ was present throughout the bed, due to the relative absence of $Fe(III)$ flocks in the water. The same reasoning could possibly justify the higher As removal efficiency observed, when no filtrate recirculation was applied. In particular, the more concentrated stream (feed of 5 m/h) appears to be more capable of directly adsorbing the formed $As(V)$, as compared to the diluted stream (2.5 m/h + 2.5 m/h). Especially, this applied at pH 7.1, in which case nearly no $As(V)$ could be found throughout the filter bed. What is more, a much higher total As removal could be achieved as compared to the diluted stream at pH 7.1 (80.8% versus 56.8%, respectively). In a nutshell, it seems that the dilution effect imposed by the recirculated filtrate had a negative effect as far as total As removal is concerned, despite the fact that a gradual Fe capturing profile over the bed height was obtained.

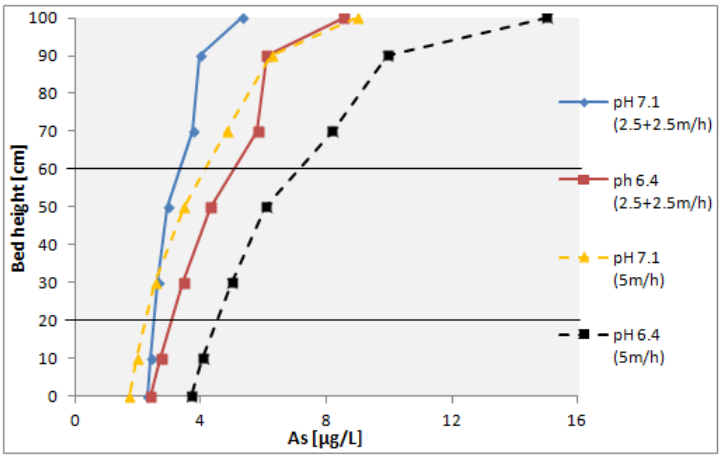

Figure 4.6: Total As concentration profiles over the different columns when 5 m/h filtration velocity with (solid curves) and without (dashed curves) filtrate recirculation was applied

4.5. Effect of different filter media on As and Fe removal

In this part, the effect of the triple layer bed (anthracite-sand-garnet) on As and Fe removal as compared to the respective effect of a single layer bed (coarse sand) is investigated. The filtration velocity of the two mixed-layer duos (running at pH 7.1 and 6.4, respectively) as well as of the single-layer duo was set at 2.5 m/h. Initially, the single-bed columns run at pH 7.1 for one week, during which four samplings took place and afterwards at pH 6.4 for a five-day period, during which three samples were collected and analyzed. Concerning the multimedia duos, three samplings were done for each one of them, over a single-week period. For each case, the duplicate columns results (of each duo), along with the different measurements over the different days were averaged and plotted in Figures 4.7 and 4.8, depicting total Fe and As concentration profiles, respectively. Figure 4.7 clearly displays the variations in Fe distributions over the filter beds between the triple- and single-bed columns. Noticeably, Fe was largely retained in the top part of the sand filters. This was also the reason, that sand columns were much more rapidly clogged and overflowed. On the other hand, Fe removal inside the multimedia filters appears to be significantly more gradual. More specifically, in the first 10 cm of the sand filters Fe had been removed by 87.2% and 59.4%, at pH 7.1 and 6.4, respectively. When we consider the triple-layer filters, the corresponding removal percentages drop to 45.3% and 37.1%, respectively.

Figure 4.8 reveals for the case of the single-layer bed a similar As removal pattern as for the Fe

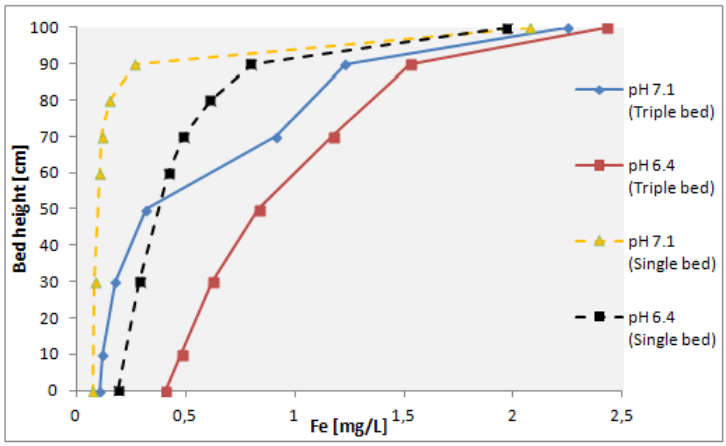

Figure 4.7: Total Fe concentration profiles when 2. 5 m/h filtration velocity was applied over mixed-bed (solid curves) and single-bed (dashed curves) filter duos

removal. Namely, most of the As was adsorbed in the top 10 cm of the bed, which was apparently driven by the fact that most of the iron was also accumulated in the same top part. After 20 cm depth, nearly no As adsorption was taken place anymore, since only a minor amount of Fe was present as well. A graph illustrating the As speciation over the single-bed height is presented in Appendix F. It appears, that although As oxidation continued over the complete bed, total As retention stopped in the first 10 – 40 cm. At pH 6.4, an enhanced As removal occurred, possibly related to the deeper Fe penetration in the sand column (heterogeneous reaction). As far as the triple-bed filter is concerned, As removal happened more gradually following the respective Fe pattern. Moreover, as observed from the As speciation graph (see Appendix F), almost no $As(V)$ could be detected (especially at pH 7.1), due to its direct adsorption by the HFOs, spread along the columns height. All in all, it comes out that the Fe dispersion over the entire height of the filter bed positively affected As removal. More precisely, single-bed filters reached total As removal of 54.1% and 81.6%, at pH 7.1 and 6.4 respectively, while the corresponding As removal efficiencies obtained by the mixed-bed columns were 88.3% and 87.5%, respectively.

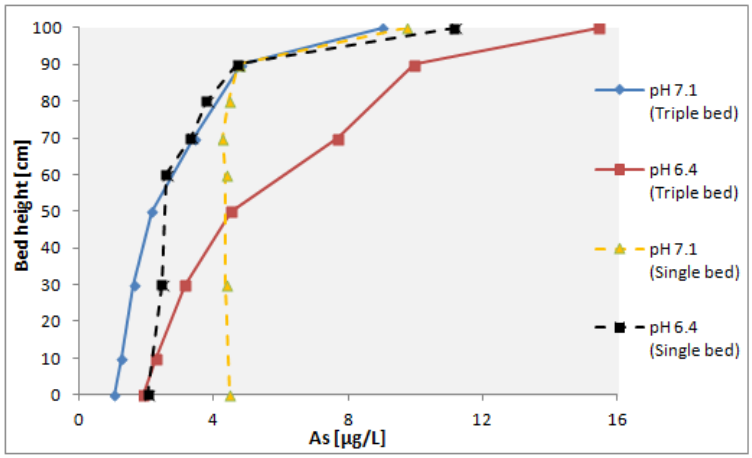

Figure 4.8: Total As concentration profiles when 2. 5 m/h filtration velocity was applied over mixed-bed (solid curves) and single-bed (dashed curves) filter duos

4.6. Disinfection of the triple-bed columns

As was previously mentioned, during the last week of the experimental process, chlorinated water was dosed to the mixed-bed columns for a two-day period. The objective was to disinfect the beds, in order

to confirm the biological nature of the undergone As oxidation. However, the results obtained from samples collected during the third and fourth day of chlorination could not be used for the drawing of reliable conclusions. According to them, As oxidation continued to take place even after two days of disinfection. Insufficient dosage of chlorine or short chlorination period could constitute reasonable explanations for the aforementioned results.

4.7. Particles volume concentration measurements

Complementary to the previously presented Fe and As concentrations analysis, some indicative particle counter measurements were conducted as well, by means of a 10-channel particle counter from PAMAS. The purpose was to acquire information regarding Fe flocs size and subsequently to get an estimation of the occurred flocculation process. Figures 4.9, 4.10 and 4.11 present the particles volume concentration, measured in the influent and the effluent of the filter beds, for the cases of 5 m/h (only feed flow), 2.5 m/h (only feed flow) and 5 m/h (feed and recirculation flow), respectively. The samples used for that series of measurements were the exact same unfiltered samples which used for the total Fe determination as well. The results provided in the following figures were based on averaged values calculated per each duo (pair of duplicate columns). One measurement was carried out in the case of the Figures 4.9 and 4.10, whereas two measurements (which were averaged) in the case of Figure 4.11.

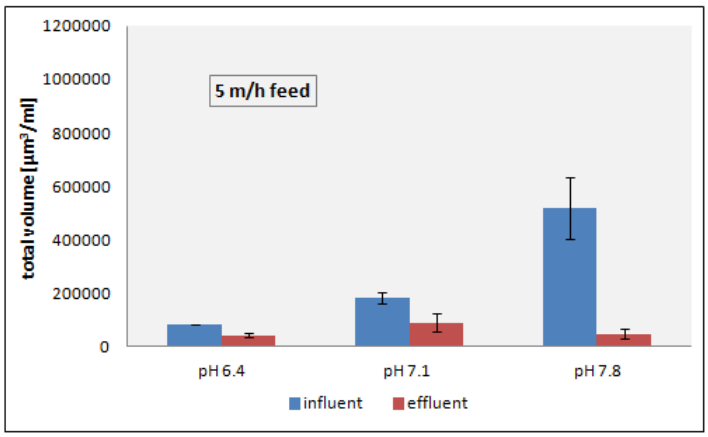

Figure 4.9: Total particles volume concentrations in the influent and effluent of the columns at pH 6.4, 7.1 and 7.8 and under feed flow 5 m/h

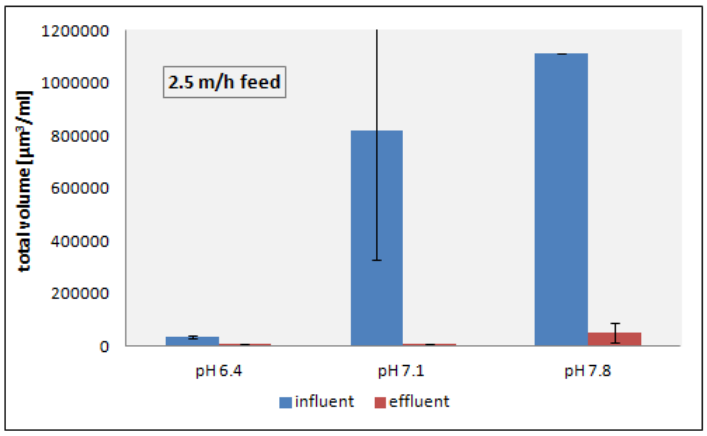

Figure 4.10: Total particles volume concentrations in the influent and effluent of the columns at pH 6.4, 7.1 and 7.8 and under feed flow 2.5 m/h

Comparison of the illustrated graphs highlights the clear tendency for larger forming flakes at higher pH values, for every filtration velocity tested. This fact could be apparently attributed to the faster oxida-

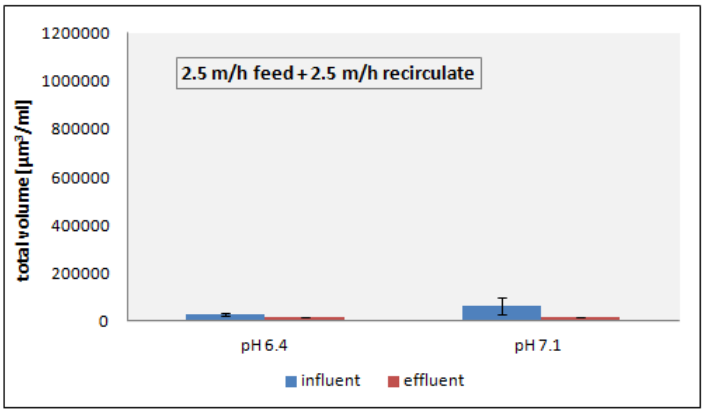

Figure 4.11: Total particles volume concentrations in the influent and effluent of the columns at pH 6.4 and 7.1 and under feed flow 2.5 m/h plus 2.5 m/h of recirculated flow

tion rates at the high pH values. In addition, in the pH range between 7 and 8 no electrostatic repulsion takes place between the iron particles, which allows for the formation of bigger flakes. When looking at the various flow rates, the largest flocs were formed when the lowest filtration velocity (2.5 m/h) was applied, which can be correlated with the longer residence and contact times of Fe in the supernatant water, as compared to the faster filtration speed (5 m/h). Under those slow flow rate conditions, sufficient time was provided for both the oxidation of dissolved Fe as well as for the subsequent particles' flocculation. Last but not least, in the case of the combined flow rate, the emerged flakes were evidently the smallest ones. Two parameters were responsible for the above outcome. On the one hand, filtration velocity was high enough (5 m/h) to allow for sufficient Fe oxidation. On the other hand, as was discussed previously, Fe concentration in the combined stream was essentially halved. As a result, less Fe mass was available for flocculation per ml of water.

4.8. Optical microscope analysis

After the termination of the entire experimental process, the columns were emptied and some representative samples of filter grains were collected (from both the single- and triple-layer beds) in order to be analyzed with the optical microscope. In Figure 4.12, two optical microscope images of sand grains collected from the top and bottom part of a single-layer bed are depicted. The brown-reddish color in the left image comprises a clear indication of the existence of Fe oxides onto the grains coating. This was the result, as previously explained, of the accumulation of the captured Fe in the top layer of the sand columns, while only a minor part of it managed to reach deeper in the bed.

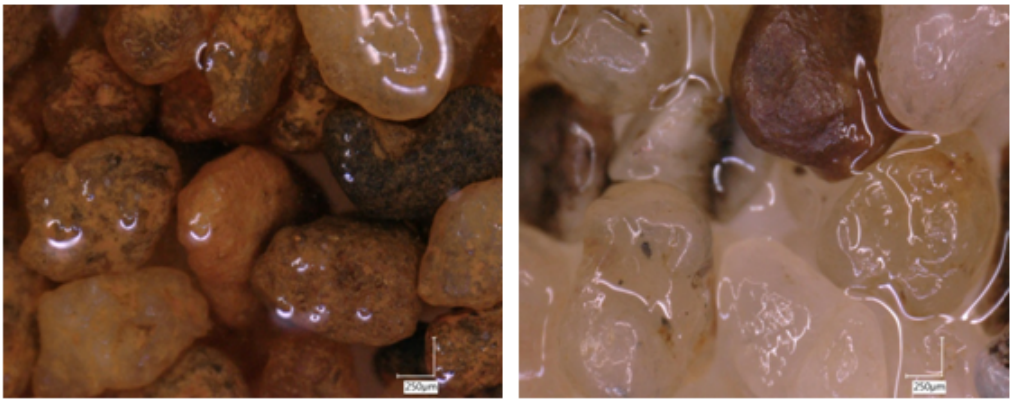

Figure 4.12: Optical microscope images of sand grains extracted from the top (left) and the bottom (right) part of a single-layer bed column

Figure 4.13 shows optical microscope images extracted from two mixed-layer columns, operating at pH 7.1 and 6.4, respectively. Representative samples were taken throughout the beds height, thus anthracite, sand and garnet grains were obtained and analyzed. Although in that occasion the differences are not so glaringly obvious, yet some variations can be observed, especially for the sand and garnet grains. More specifically, for pH 6.4 (bottom images) a more intense red-brownish coating can be observed in both sand and garnet grains, as compared to the respective grains for pH 7.1 (top images). In contrast, significant discrepancies between the anthracite grains cannot be observed. The variation in the coloring of sand and garnet grains potentially originated from the different prevailed Fe removal mechanisms, which took place in those columns. As seen above, at pH 6.4 mainly the heterogeneous Fe removal mechanism dominated, which resulted in the creation of a an iron oxide coating around the medium grains. This was not the case for pH 7.1, in which all the Fe already entered the filter bed as HFO particles. Lastly, an additional potential reason explaining the different grains coloring between the two columns, may come from the different Fe concentrations present in the part of the beds, from which the samples were extracted. In this case, higher Fe concentrations throughout the bed were observed at pH 6.4 than at pH 7.1 (filtration velocity 2.5 m/h).

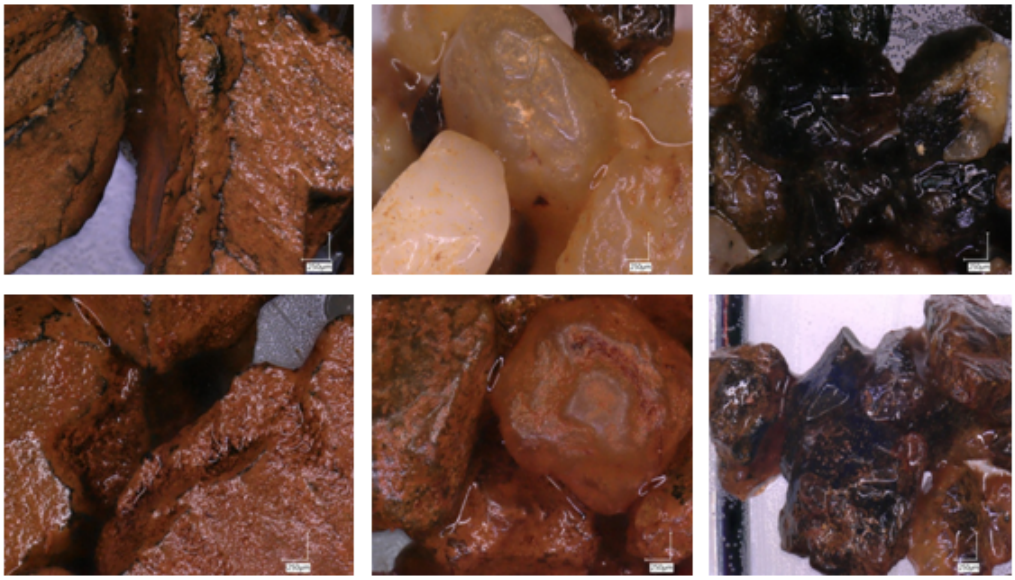

Figure 4.13: Optical microscope images of anthracite, sand and garnet grains extracted from mixed-layer bed columns operated at pH 7.1 (top row) and pH 6.4 (bottom row)

5

Conclusions

The current study revealed the superiority of the triple-layer against single-layer filters in terms of deep Fe bed penetration as well as in terms of effective As removal. Additionally, significantly longer filter run times were achieved by the multimedia filters. Different operational settings were tested. The results revealed that As removal was evidently favored by the relatively high pH levels (7.1 and 7.8) and the rapid formation of $Fe(III)$ flocks which effectively absorbed $As(V)$. The deeper penetration of the formed flakes throughout the entire filter column displays a beneficial impact regarding As retention. On the other hand, at the lower pH value 6.4, the predominant Fe removal mechanism comprised the adsorption-oxidation mechanism, which seemed to disrupt the proper functioning of the AsOB on the filter grains. Furthermore, it was confirmed that the oxidized As form $(As(V))$ adsorbs more efficiently onto the HFO than the reduced form $As(III)$. Last but not least, the different examined filtration velocities (2.5 m/h and 5 m/h) did not appear to have an important effect on As removal at the high pH values, whereas the filtrate recirculation back to the inlet of the filter column did not exhibit a positive influence towards a sufficient As retention. Finally, the current study contributed to a more thorough understanding of the influence that the aforementioned operational settings can have on the concurrent removal of As and Fe ions from groundwater, towards an improved biological rapid sand filtration.

Bibliography

[1] Vewin. “Dutch Drinking Water Statistics 2017 From source to tap”. In: *Journal of Water and Health, 15(1)* (2017), pp. 81–85.

[2] Ş. Şener, E. Şener, and A. Davraz. “Assessment of groundwater quality and health risk in drinking water basin using GIS”. In: *Journal of Water and Health, 15(1)* (2016), pp. 112–132.

[3] H. Nash and G.J.H. McGall. “Groundwater Quality - 17th Special Report Chapman Hall”. In: (1994).

[4] Eawag. “Geogenic Contamination Handbook - Addressing Arsenic and Fluoride in Drinking Water”. In: (Dübendorf, Switzerland: Swiss Federal Institute of Aquatic Science and Technology.2015).

[5] T. Harter. “Groundwater Quality and Groundwater Pollution”. In: (Oakland, California: University of CaliforniaAgriculture and Natural Resources.2016).

[6] J. Gude, L. Rietveld, and D. van Halem. “Fate of low arsenic concentrations during full-scale aeration and rapid filtration”. In: *Water Research, 88* (2016), pp. 566–574.

[7] P. Smedley and D. Kinniburgh. “A review of the source, behaviour and distribution of arsenic in natural waters”. In: *Applied Geochemistry, 17(5)* (2002), pp. 517–568.

[8] Md. Safiuddin. “Arsenic contamination of groundwater in Bangladesh: A review”. In: *International Journal of the Physical Sciences, 6(30)* (2011).

[9] D. Chakraborti et al. “Status of groundwater arsenic contamination in Bangladesh: A 14-year study report”. In: *Water Research, 44(19)* (2010), pp. 5789–5802.

[10] A. Duarte, S. Cardoso, and A. Alçada. “Emerging and Innovative Techniques for Arsenic Removal Applied to a Small Water Supply System”. In: *Sustainability, 1(4)* (2009), pp. 1288–1304.

[11] R. Ratnaike. “Acute and chronic arsenic toxicity”. In: *Postgraduate Medical Journal, 79(933)* (2003), pp. 391–396.

[12] S. Lamm et al. “Arsenic in Drinking Water and Bladder Cancer Mortality in the United States: An Analysis Based on 133 U.S. Counties and 30 Years of Observation”. In: *Journal of Occupational and Environmental Medicine, 46(3)* (2004), pp. 298–306.

[13] WHO. “Guidelines for drinking-water quality Guidelines for drinking-water quality - 4th ed. World Health Organization”. In: (2011).

[14] EPA. “2018 Edition of the Drinking Water Standards and Health Advisories Tables.” In: (Washington, DC: Office of Water U.S. Environmental Protection Agency.2018).

[15] S. KAPAJ et al. “Human Health Effects From Chronic Arsenic Poisoning–A Review”. In: *Journal of Environmental Science and Health, Part A, 41(10)* (2006), pp. 2399–2428.

[16] S. Bordoloi, M. Nath, and R. Dutta. “pH-conditioning for simultaneous removal of arsenic and iron ions from groundwater.” In: *Process Safety and Environmental Protection, 91(5)* (2013), pp. 405–414.

[17] P. Mondal et al. “Remediation of inorganic arsenic in groundwater for safe water supply: A critical assessment of technological solutions.” In: *Chemosphere, 92(2)* (2013), pp. 157–170.

[18] M. SHAFIQUZZAMAN, I. MISHIMA, and J. NAKAJIMA. “Arsenic Removal from Ground Water by Sand Filtration during Biological Iron Oxidation.” In: *Japanese Journal of Water Treatment Biology, 44(1)* (2008), pp. 11–20.

[19] S. Vigneswaran and C. Visvanathan. “Water treatment processes”. In: *Boca Raton: CRC Press* (1995), pp. 156–157.

[20] K. Teunissen et al. “Removal of both dissolved and particulate iron from groundwater”. In: *Drinking Water Engineering and Science Discussions, 1(1)* (2008), pp. 87–115.

[21] UNITED STATES DEPARTMENT OF THE INTERIOR. “Survey of Ferrous-Ferric Chemical Equilibria and Redox Potentials”. In: *Drinking Water Engineering and Science Discussions, 1(1)* (Washington,1959), pp. 4–7.

[22] P. Mouchet. “From Conventional to Biological Removal of Iron and Manganese in France.” In: *Journal - American Water Works Association, 84(4)* (1992), pp. 158–167.

[23] S. Sharma. “Adsorptive Iron Removal from Groundwater”. In: *Doctor. Wageningen University.* (2001).

[24] S. Sharma et al. “Comparison of physicochemical iron removal mechanisms in filters”. In: *Journal of Water Supply: Research and Technology-Aqua, 50(4)* (2001), pp. 187–198.

[25] C. Lerk. “Enkele aspecten van de ontijzering van grondwater”. In: *Phd. Technical University Delft.* (1965).

[26] W. Stumm and J. Morgan. In: *Aquatic Chemistry. Third Edition. John Wiley Sons Inc., USA.* (1996).

[27] W. Stumm and G. Lee. In: *Oxygenation of ferrous iron. Industrial Engineering and Chemistry, 53(2)* (1961), pp. 143–146.

[28] H. Tamura, K. Goto, and M. Nagayama. In: *The effect of ferric hydroxide on the oxygenation of ferrous ions in neutral solutions. Corrosion Science, 16* (1976), pp. 197–207.

[29] N. Tufekci and H. Sarikaya. In: *Catalytic effects of high fe(iii) concentrations on fe(ii) oxidation. Water Science and Technology, 34(7-8)* (1996).

[30] Sarikaya. In: *Contact aeration for iron removal—A theoretical assessment. Water Research, 24(3)* (1990), pp. 329–331.

[31] E. Søgaard, R. Medenwaldt, and J. Abraham-Peskir. In: *Conditions and rates of biotic and abiotic iron precipitation in selected Danish freshwater plants and microscopic analysis of precipitate morphology. Water Research, 34(10)* (2000), pp. 2675–2682.

[32] J. O’Connor. In: *Iron and Manganese. Water Quality and Treatment - A Handbook of Public Water Supplies, Chapter 11* (1971), pp. 378–396.

[33] C. Van Beek et al. In: *Contributions of homogeneous, heterogeneous and biological iron(II) oxidation in aeration and rapid sand filtration (RSF) in field sites. Journal of Water Supply: Research and Technology-Aqua, 65(3)* (2015), pp. 195–207.

[34] J. Wilkie and J. Hering. In: *Adsorption of arsenic onto hydrous ferric oxide: effects of adsorbate/adsorbent ratios and co-occurring solutes. Colloids and Surfaces A: Physicochemical and Engineering Aspects, 107* (1996), pp. 97–110.

[35] S. Dixit and J. Hering. In: *Comparison of Arsenic(V) and Arsenic(III) Sorption onto Iron Oxide Minerals: Implications for Arsenic Mobility. Environmental Science Technology, 37(18)* (2003), pp. 4182–4189.

[36] J. Gude, L. Rietveld, and D. van Halem. In: *As(III) oxidation by MnO 2 during groundwater treatment. Water Research, 111* (2017), pp. 41–51.

[37] M. Bissen and F. Frimmel. In: *Arsenic— a Review. Part II: Oxidation of Arsenic and its Removal in Water Treatment. Acta hydrochimica et hydrobiologica, 31(2)* (2003), pp. 97–107.

[38] J. Gude, L. Rietveld, and D. van Halem. “Biological As(III) oxidation in rapid sand filters.” In: *Journal of Water Process Engineering, 21,* (2017), pp. 107–115.

[39] A. Voegelin and S. Hug. “Catalyzed Oxidation of Arsenic(III) by Hydrogen Peroxide on the Surface of Ferrihydrite: An in Situ ATR-FTIR Study.” In: *Arsenic— a Review. Part II: Oxidation of Arsenic and its Removal in Water Treatment. Acta hydrochimica et hydrobiologica, 31(2)* (2003), pp. 972–978.

[40] K. Amstaetter et al. “Redox Transformation of Arsenic by Fe(II)-Activated Goethite (α-FeOOH).” In: *Environmental Science Technology, 44(1)* (2010), pp. 102–108.

[41] J. Gude, L. Rietveld, and D. van Halem. “As(III) removal in rapid filters: Effect of pH, Fe(II)/Fe(III), filtration velocity and media size.” In: *Water Research, 147,* (2018), pp. 342–349.

[42] A. Stefánsson. “Iron(III) Hydrolysis and Solubility at 25 °C.” In: *Environmental Science Technology, 41(17),* (2007), pp. 6117–6123.

A

Appendix

A.1.

The rate of the heterogeneous reaction can be described by equation A.1 [28]:

$$\textit{Heterogeneous reaction rate}: \frac{-d[Fe(II)]}{dt} = (k + k \cdot Fe[III]) \cdot [Fe(II)] \quad \text{(A.1)}$$

where, k is the rate constant of the homogeneous iron oxidation (M/min), k' is the rate constant of the heterogeneous reaction $k_{so}[O2]K/[H^+]$, k_{so} is the real rate constant of the heterogeneous reaction (M) and K is the equilibrium constant for the adsorption of $Fe(II)$ on $Fe(III)$ hydroxide

A.2.

$Fe(III)$ speciation as a function of the pH [42].

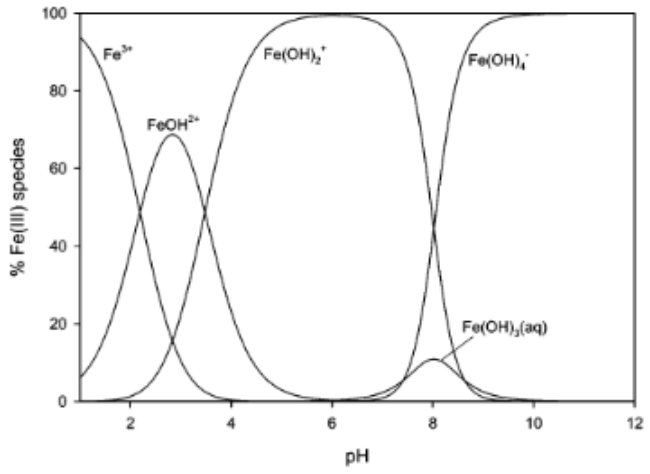

A.3.

Total As and $As(III)$ concentrations over the filter bed height of the three examined duos (every duo was operated at a different pH value). The filtration velocity was 5 m/h. Data presented here are averaged values of three sampling measurements over a seven-week period.

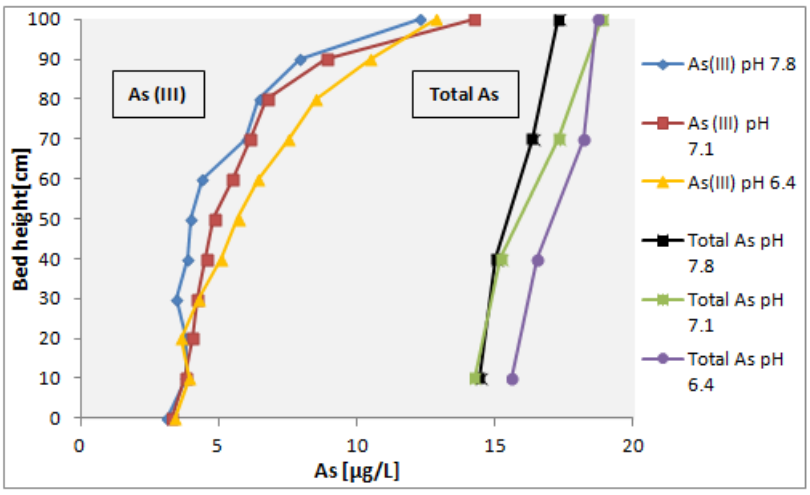

B

Appendix

Total Fe and $Fe(II)$ concentrations along the bed height at different pH values. The applied filtration velocity was 5 m/h. Data presented here are averaged values of 4 sampling measurements over a ten-day period.

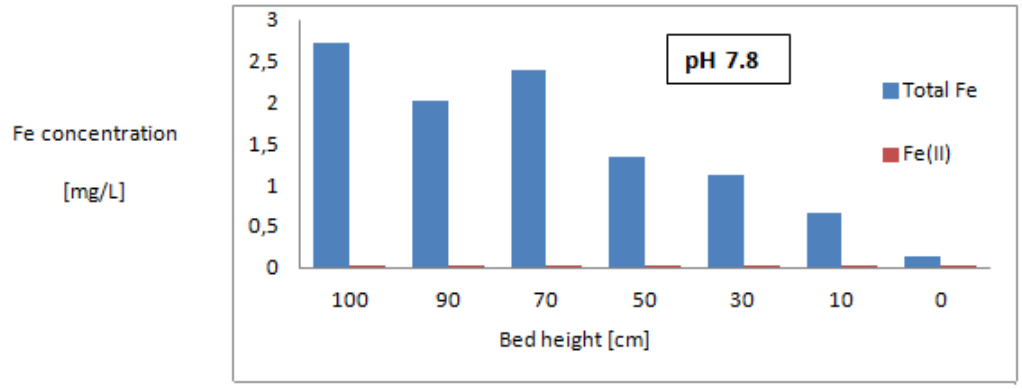

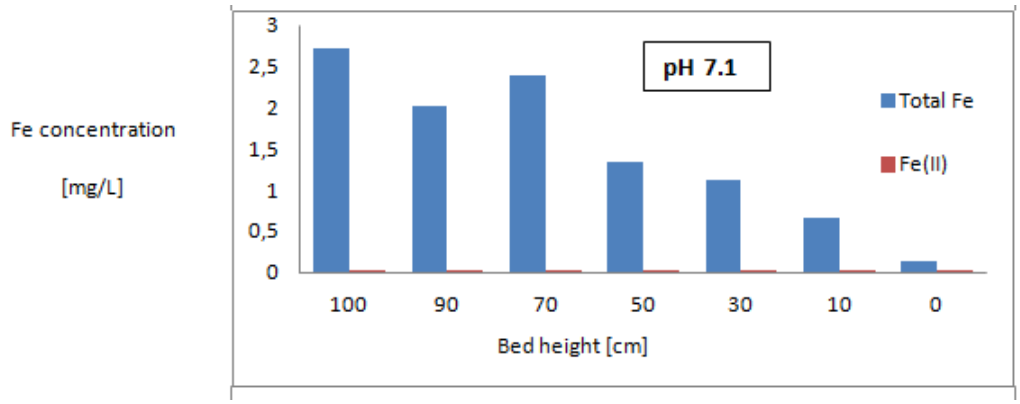

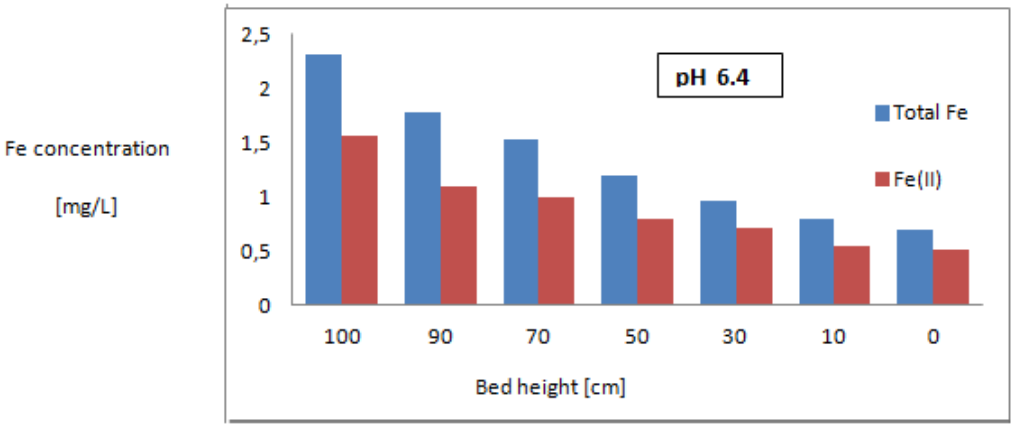
Fe concentration
[mg/L]
2,5
2
1,5
1
0,5
0
pH 6.4
Total Fe
Fe(II)
100
90
70
50
30
10
0
Bed height [cm]

C

Appendix

Total As and $As(III)$ concentrations along the bed height at different pH values. The filtration velocity was 5 m/h. Data presented here are averaged values of 4 sampling measurements over a ten-day period.

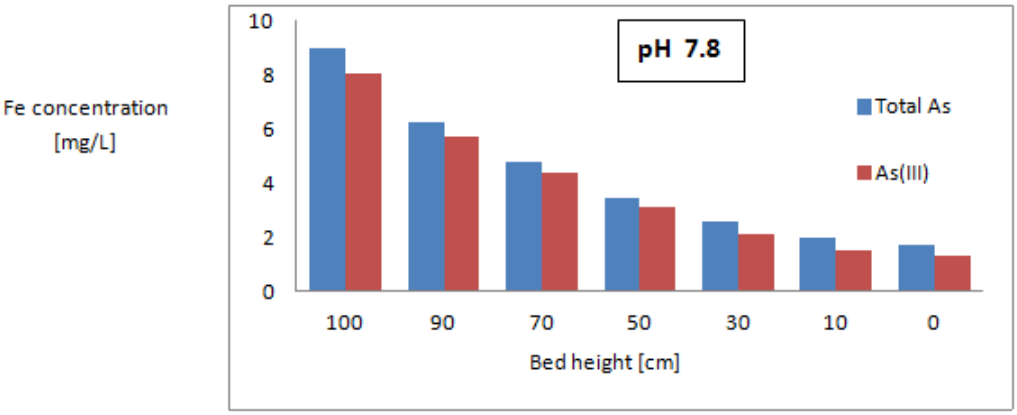

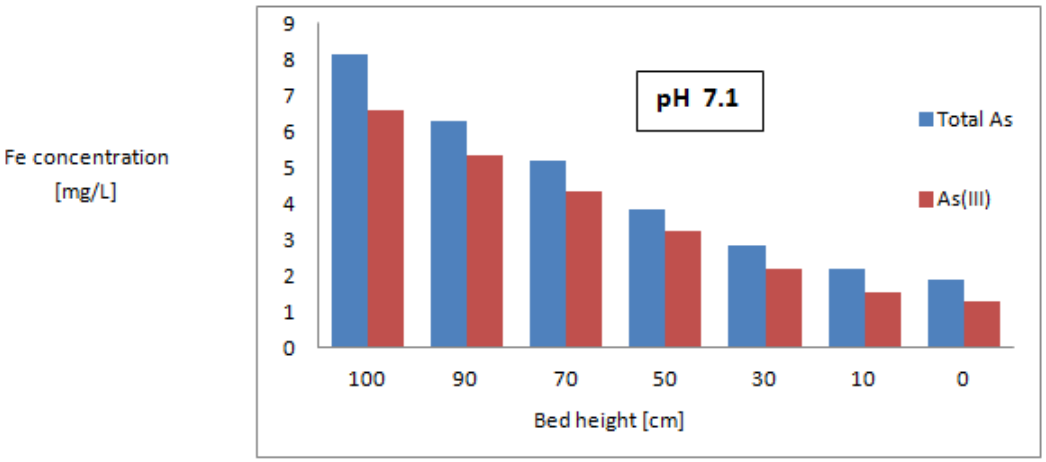

Fe concentration
[mg/L]

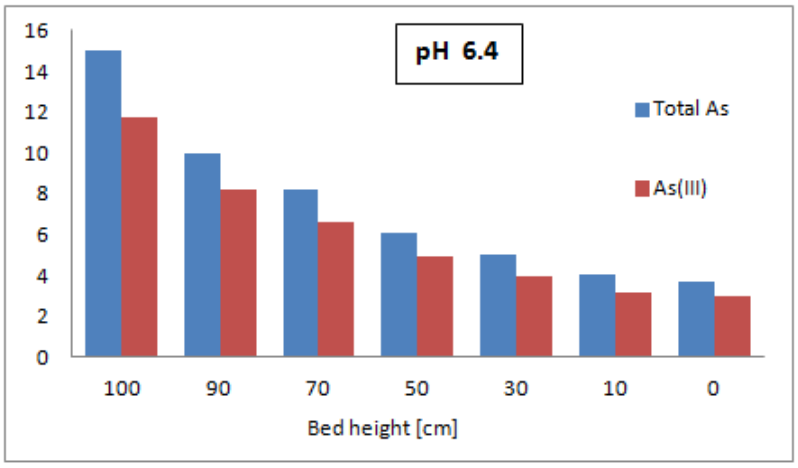

D

Appendix

Direct comparison of the total Fe concentration profiles for 2.5 m/h and 5 m/h applied flow rate, at the three examined pH values.

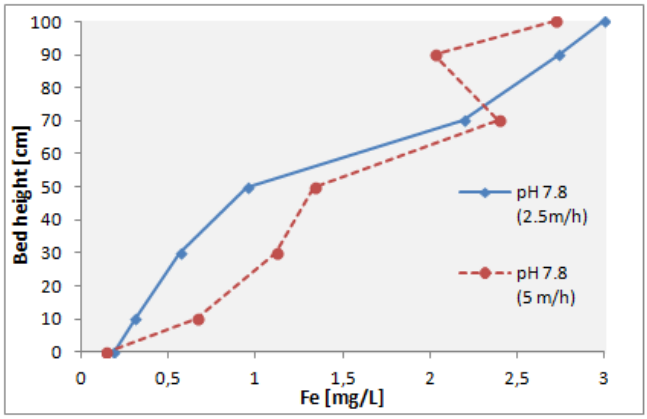

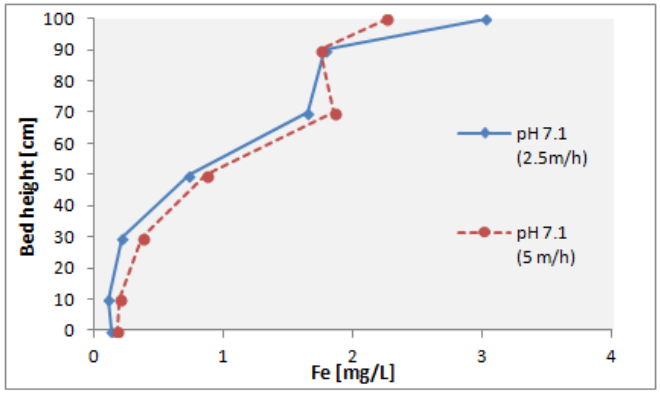

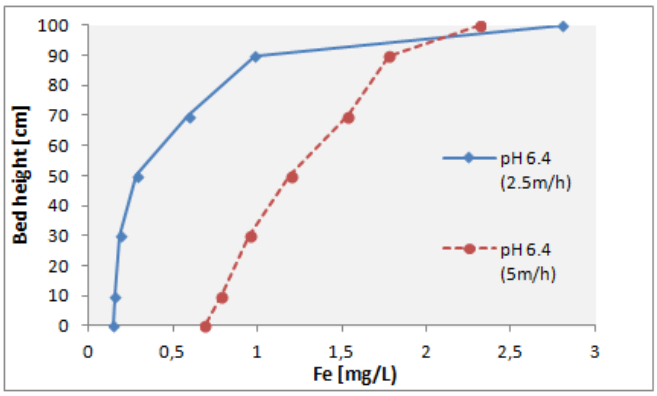

Direct comparison of the total As concentration profiles for 2.5 m/h and 5 m/h applied flow rate, at the three examined pH values.

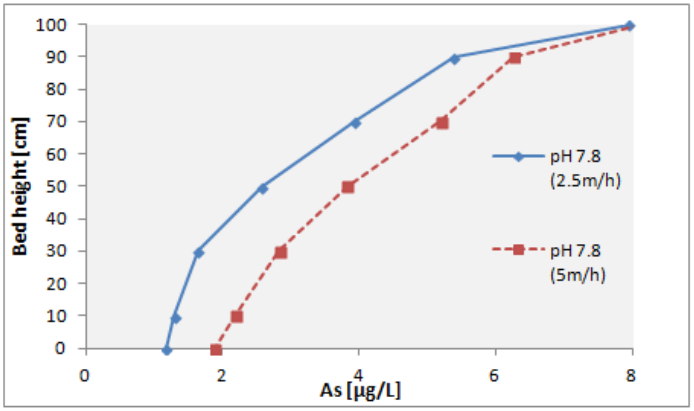

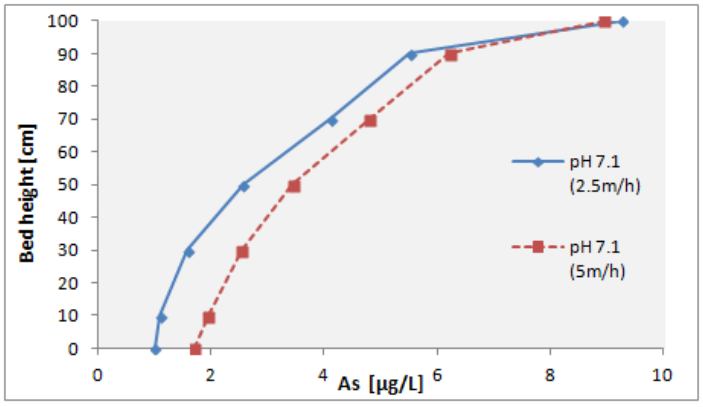

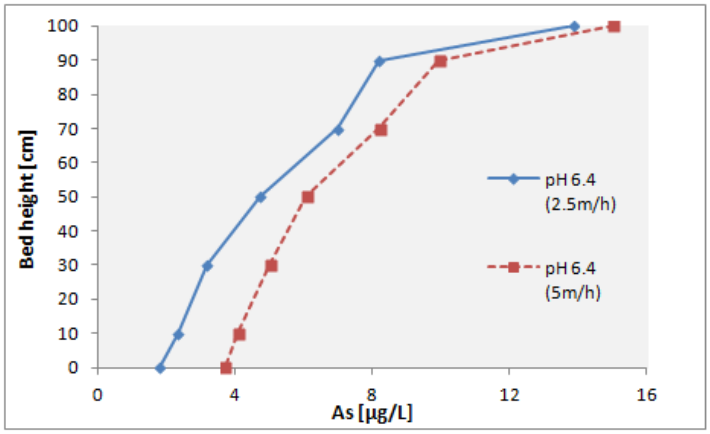
Bed height [cm]
100
90
80
70
60
50
40
30
20
10
0
0
4
8
12
16
As [µg/L]
pH 6.4
(2.5m/h)
pH 6.4
(5m/h)

E

Appendix

Total Fe and $Fe(II)$ concentration along the filter bed at pH 7.1 and 6.4, when the total flow (5m/h) consists of both the feed and the recirculated flow.

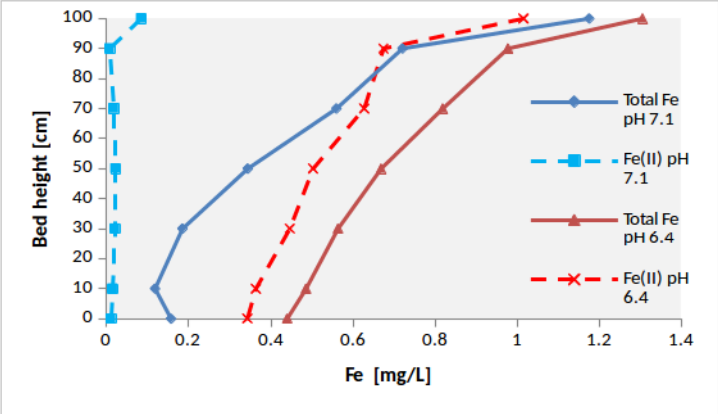

As speciation graphs at both pH 7.1 and 6.4 when part of the filtrate is recirculated.

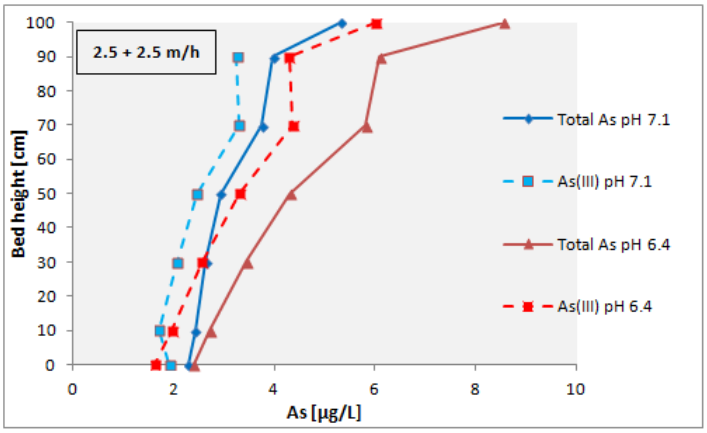

As speciation graphs for both pH 7.1 and 6.4 without recirculation.

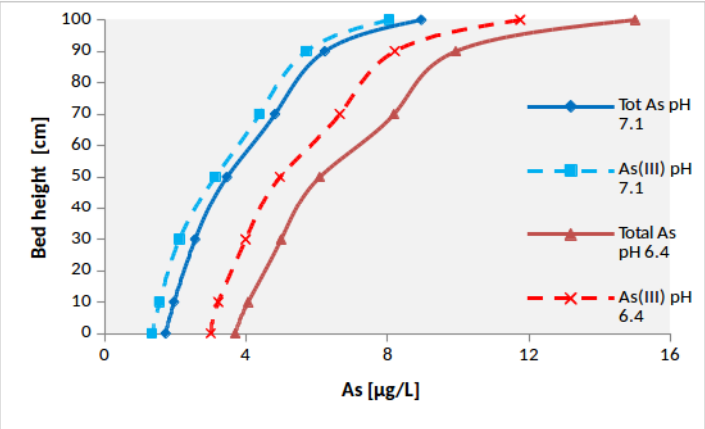

Appendix

As speciation graphs at both pH 7.1 and 6.4 for the single-layer bed case.

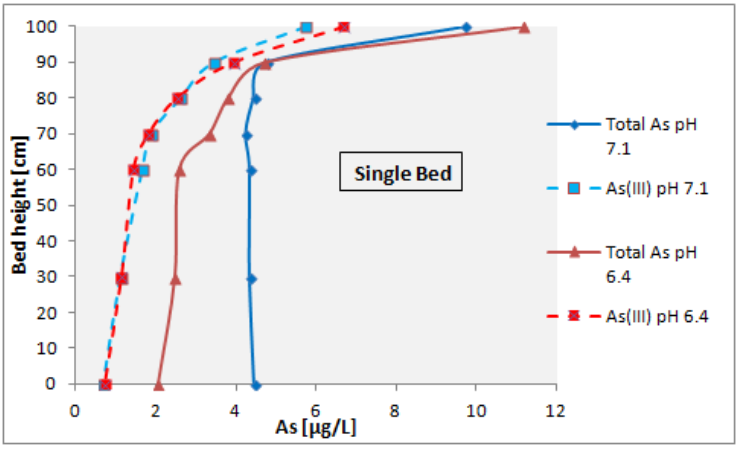

As speciation graphs at both pH 7.1 and 6.4 for the triple-layer bed case.